IJARSCT
International Journal of Advanced Research in Science, Communication and Technology
International Open-Access, Double-Blind, Peer-Reviewed, Refereed, Multidisciplinary Online Journal
ISSN: 2581-9429
Volume 6, Issue 4, October 2026
Impact Factor: 8.2

Influence of Cobalt Substitution on the Structural, Morphological, and Magnetic Properties of Magnesium Spinel Ferrite

Ajay Yoel[1], Lalit D. Channe[1], Shrikant M. Suryawanshi[2]
[1]Department of Physics, Hislop College, Nagpur, India
[2]Department of Physics, Kamla Nehru Mahavidyalaya, Nagpur, India
[1]lalitchanne74@gmail.com

Abstract: *Mix magnesium cobalt nanoferrites, Mg1-xCoxFe2O4 (x = 0, 0.2) synthesized via chemical co-precipitation route to investigate the influence of Co2+ substitution on their structural, optical, magnetic and morphological properties. X-ray diffraction pattern (XRD) reveals the formation of single-phase cubic spinel structure belonging to Fd3m space group. With the introduction 20% cobalt (x = 0.2), the lattice parameter expanded from 0.8357 nm to 0.8374 nm and crystallite size increased from 20.14 nm to 34.46 nm, which is attributed to substitution of host Mg2+ with larger Co2+ ions. Fourier transform infrared (FTIR) spectroscopy displayed two primary metal-oxygen vibrational bands corresponding to tetrahedral site increased from 536.23 cm-1 to 670.29 cm-1 and octahedral site from 454.26 cm-1 to 491.87 cm-1 with the substitution of cobalt ion demonstrate increased in bond stiffness and force constant. Transmission electron microscopy (TEM) showed polygonal geometries with narrow size distribution and average particle size of 20.63 nm for Mg0.8Co0.2Fe2O4. Vibrating sample magnetometry (VSM) shows standard ferrimagnetic behavior, where Co2+ incorporation into the octahedral sites strengthened the inter-sublattice exchange coupling and boosted saturation magnetization (MS) from 15.15 emu/g to 21.15 emu/g and remanent magnetization (Mr) from 3.92 emu/g to 5.83 emu/g. Concurrently, the strong single-ion magneto crystalline anisotropy of cobalt increased coercivity (HC) from 189.96 Oe to 239.10 Oe and anisotropy constant (K) from 2997.80 erg/g to 5267.67 erg/g. These structural and magnetic enhancements highlight the suitability of these nanoferrites for high-frequency electronics, magnetic storage devices, and biomedical applications such as MRI contrast agents and magnetic hyperthermia.*

Keywords: XRD, FTIR, VSM, TEM, nanoferrites

I. INTRODUCTION

Ferrite is a ceramic material consisting of iron oxide (Fe2O3) with one or more metallic elements such as Ni, Cu, Zn, Mg, Co or Mn [1]. Ferrites are classified as soft or hard based on their magnetic properties dependent on the coercivity of the material. Based on their crystal structure ferrites are classified into spinel, hexagonal, garnet and ortho ferrite. Among them, spinel ferrites have a face-cantered cubic (FCC) structure with a general formula MFe2O4, where M is a divalent metal ion such as Ni, Cu or Co [2]. Spinel ferrites have high electrical resistivity, low eddy current losses and thermal and chemical stability. These materials are utilized in high-frequency devices, electromagnetic interference (EMI) shielding, high-density magnetic recording, and targeted drug delivery [3]. In Mg-Co ferrite, a spinel ferrite, the cobalt substitution results in a cubic spinel lattice with improved chemical bond stiffness and larger crystallite size. This material shows high electrical resistivity, lower eddy current losses and chemically tuned ferrimagnetism with higher saturation magnetization, coercivity and magneto crystalline anisotropy due to the occupation of Co2+ ions in octahedral sites [4]. At the nanoscale, Mg-Co ferrite's high chemical stability, narrow particle size distribution, and

IJARSCT
International Journal of Advanced Research in Science, Communication and Technology
International Open-Access, Double-Blind, Peer-Reviewed, Refereed, Multidisciplinary Online Journal
ISSN: 2581-9429
Volume 6, Issue 4, October 2026
Impact Factor: 8.2

moderated squareness ratio make it suitable for high-frequency electronics, magnetic storage, and biomedical hyperthermia applications [5].

II. LITERATURE REVIEW

Much attention has been paid by the researchers to Mg–Co spinel ferrites due to their tunable structural, magnetic, electrical and dielectric properties. For example, Mohammad et al. [6] synthesized Co1-xMgxFe2O4 nanoparticles by the sol-gel auto-combustion method and observed that the saturation magnetization, remanence and coercivity gradually decreased with increasing Mg2+ substitution, which has been attributed to the filling of Mg2+ ions in octahedral positions. Vinayak et al. [7,8] have also reported similar results for the low temperature synthesized Mg2+ substituted cobalt spinel ferrite nanoparticles and have attributed the observed change in magnetic and electrical properties to the redistribution of cations. Furthering this work, Hashhash and Kaiser [9] incorporated Ca^{2+} into Mg–Co–Cr nanoferrites, revealing that Ca^{2+} at grain boundaries restricted crystallite growth to below 10 nm, while maintaining a pure spinel phase and ferromagnetic behaviour. Mondal et al. [10] studied the effect of annealing on Co–Mg spinel system and reported an increase in particle size from 8.2 to 52.15 nm and increase in coercivity with increase in annealing temperature. Chebbi et al.

[11] studied the effect of Cr3+ substitution on the structural, optical and electrical properties of Mg–Co ferrites prepared by sol–gel method. The effect of cobalt concentration on lattice expansion and dielectric behaviour was also observed by Malik et al. [12] in Mg1-xCoxFe2O4 nanoferrites prepared by co-precipitation method. In addition, rare-earth element doping has been explored. Belaiche et al. [13] synthesized the Gd^{3+} doped Co-Mg ferrite nanoparticles by coprecipitation and confirmed the single-phase cubic spinel structure and characteristic vibrations of the sites by FTIR. Huang et al. [14] studied La^{3+} doped $Mg_{0.2}Co_{0.8}Fe_{2-x}LaxO4$, with coercivity values in the range of 611 - 779 Oe, exhibiting characteristics of hard magnetic behaviour. Kuswanth kumar et al. [15] reported Cu2+ -doped Mg-Co ferrites prepared by solid state reaction method exhibited gradual decrease in DC electrical resistivity with the increase in Cu2+ content while maintaining the spinel phase. Altogether, these studies highlight the adaptability of Mg–Co spinel ferrites for tailoring magnetic and dielectric properties through careful control of composition and doping strategies.

III. RESEARCH METHODOLOGY

MgFe2O4 and Mg0.8Co0.2Fe2O4 nanoferrites have been prepared by chemical co-precipitation method and their structural and magnetic properties have been investigated. The starting materials used were analytical reagent (AR) grade Magnesium Chloride (MgCl2), Cobalt Chloride (CoCl2), Ferric Chloride (FeCl3) and Sodium Hydroxide (NaOH). The chemicals were dissolved in 40 ml distilled water in stoichiometric ratio 1:2 and stirred at 60°C for 20 min. Dropwise addition of NaOH was used to adjust the solution to pH 12 so as to facilitate the precipitation. The obtained mixture was stirred and heated continuously during about 1 h and 30 min. After cooling, the precipitate was separated by filtration and washed several times with distilled water and ethanol to remove any residual impurities. The obtained precipitate was then dried in an oven for approximately 2 hours at 100°C, ground with a mortar and pestle to obtain a fine powder, and subsequently calcined at 800°C for 5 hours. The final product was further ground for about 1 hour and 30 minutes to achieve uniform particle size. The synthesized nanoferrites were then characterized using X-ray diffraction (XRD), Fourier-transform infrared spectroscopy (FTIR), transmission electron microscopy (TEM), and vibrating sample magnetometry (VSM) analysis to evaluate their structural and magnetic properties.

IJARSCT
International Journal of Advanced Research in Science, Communication and Technology
International Open-Access, Double-Blind, Peer-Reviewed, Refereed, Multidisciplinary Online Journal
ISSN: 2581-9429
Volume 6, Issue 4, October 2026
Impact Factor: 8.2

IV. RESULTS AND DISCUSSION

X-Ray Diffraction (XRD Results)

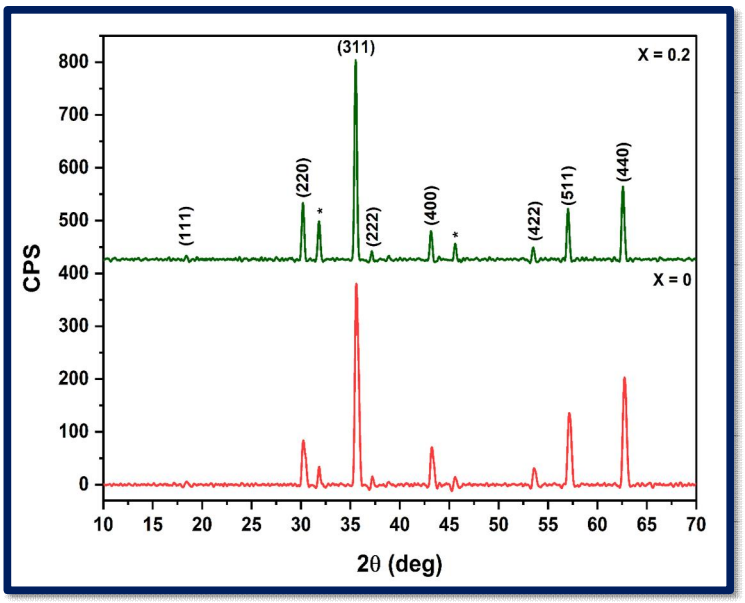


Fig 1: **XRD of $Mg_{1-x}Co_xFe_2O_4$ (x = 0, 0.2)**

Parameters	x = 0	x = 0.2
2θ (degree)	35.589	35.525
FWHM β (degree)	0.433	0.253
Crystallite Size D (nm)	20.14	34.46
d-spacing (nm)	0.2520	0.2525
Lattice constant a (nm)	0.8357	0.8374
Unit cell volume V (cm^3)	5.83×10^{-22}	5.87×10^{-22}
Tetrahedral bond length A-O(nm)	0.1809	0.1813
octahedral bond length B-O(nm)	0.2089	0.2093
Tetrahedral hopping length L_A (nm)	0.3618	0.3626
octahedral hopping length L_B (nm)	0.2954	0.2960

Table 1: **XRD Parameters for $Mg_{1-x}Co_xFe_2O_4$ (x = 0, 0.2)**

The phase purity, crystal structure, and microstructural evolution of the magnesium cobalt ferrite series, specifically $MgFe_2O_4$ (x = 0) and $Mg_{0.8}Co_{0.2}Fe_2O_4$ (x = 0.2), were investigated through systematic synthesis via the co-precipitation method. X-ray diffraction (XRD) analysis performed at room temperature for both pure and cobalt-substituted magnesium ferrite samples exhibited intense, sharp, and well-resolved Bragg peaks. These peaks corresponded to the characteristic Miller indices (111), (220), (311), (222), (400), (422), (511), and (440), which are indicative of a single-phase cubic spinel structure with Fd-3m space group symmetry. Despite the successful formation of the desired phase, a minor secondary peak was observed near $2\theta \approx 32$ degrees in both compositions, while a weak additional reflection at $2\theta \approx 45.6$ degrees was detected only in the cobalt-doped sample. The presence of these minor peaks suggests the existence of a small quantity of unreacted secondary phase, possibly arising from local stoichiometric deviations or kinetic limitations during synthesis at elevated temperatures [16].

IJARSCT
International Journal of Advanced Research in Science, Communication and Technology
International Open-Access, Double-Blind, Peer-Reviewed, Refereed, Multidisciplinary Online Journal
ISSN: 2581-9429
Volume 6, Issue 4, October 2026
Impact Factor: 8.2

To rigorously assess the structural changes induced by compositional variation, key crystallographic parameters were determined based on the most intense (311) reflection observed in the XRD patterns. Substitution of magnesium by cobalt (x = 0 to x = 0.2) resulted in a shift of the (311) peak to lower diffraction angles, changing from 35.589° to 35.525°. According to Bragg's law, this shift corresponds to an increase in the interplanar spacing (d) from 0.2520 nm to 0.2525 nm. Consequently, the lattice parameter (a) expanded systematically from 0.8357 nm to 0.8374 nm. This behavior is consistent with Vegard's law and can be attributed to the larger ionic radius of Co^{2+} compared to Mg^{2+} [17], leading to lattice expansion. The expansion of the crystal lattice is further corroborated by the increase in unit cell volume from 5.83×10^{-22} cm³ to 5.87×10^{-22} cm³.

Simultaneously a considerable drop in Full Width at Half Maximum (FWHM) values is observed from 0.433 degrees to 0.253 degrees. The reduction of the diffraction patterns according to the Scherrer equation indicates a significant change in the microstructural grain configuration leading to an increase of the average crystallite size (D) from 20.14 nm in the unmodified sample to 34.46 nm in the 20 percent cobalt substituted sample. This phenomenon shows that the introduction of cobalt ions reduces the activation energy threshold for grain boundary movement during calcination, which results in improved crystallisation of the structure and a decrease in defects in the lattice [18].

Such structural alterations at the unit cell level directly control the local internal chemical properties of the crystal lattice. The addition of cobalt causes the lengths of the tetrahedral (A-O) and octahedral (B-O) metal-oxygen bonds to grow, with the tetrahedral bond length going from 0.1809 nm to 0.1813 nm and the octahedral bond length going from 0.2089 nm to 0.2093 nm. The concurrent increase of the local environments shows that the entering cobalt ions are spread over both sublattices, leading to a general expansion of the oxygen polyhedral cages [19]. In accordance with this behaviour, the physical hopping distances, which correspond to the shortest separation between neighbouring active magnetic ions, increase for both sublattices. The tetrahedral hopping length (LA) changes from 0.3618 nm to 0.3626 nm while the octahedral hopping length (LB) changes from 0.2954 nm to 0.2960 nm. This systematic increase in hopping distances modifies the overlap of coherence between the cation 3d orbitals and the intermediate oxygen 2p orbitals, generally reducing inter-sublattice exchange coupling interactions and affecting electrical conductivity by requiring charge carriers to travel over larger spatial distances [20].

Fourier Transform Infrared Radiation (FTIR Results)

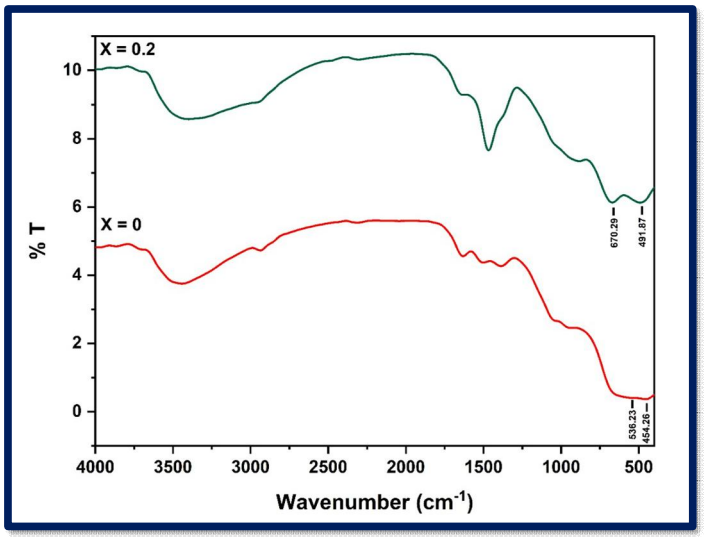


Fig 2: FTIR of $Mg_{1-x}Co_xFe_2O_4$ (x = 0, 0.2)

IJARSCT
International Journal of Advanced Research in Science, Communication and Technology
International Open-Access, Double-Blind, Peer-Reviewed, Refereed, Multidisciplinary Online Journal
ISSN: 2581-9429
Volume 6, Issue 4, October 2026
Impact Factor: 8.2

	Wavenumber (cm^{-1})		Force Constant (N/m)	
	υ (tetrahedral)	υ (octahedral)	K (tetrahedral)	K (octahedral)
x = 0	536.23	454.26	2.10×10^2	1.51×10^2
x = 0.2	670.29	491.87	3.29×10^2	1.77×10^2

Table 2: **FTIR Parameters for $Mg_{1-x}Co_xFe_2O_4$ (x = 0, 0.2)**

The Fourier transform infrared (FTIR) spectra of the synthesized $Mg_{1-x}Co_xFe_2O_4$ (where x = 0 and x = 0.2) spinel ferrite series were systematically recorded at room temperature to evaluate the local structural characteristics, vibrational modes, and site coordination modifications induced by cobalt substitution. For all compositions in this mixed system, the infrared spectra exhibit two principal metal-oxygen vibrational absorption bands in the wavenumber region below 1000 cm^{-1}, which represents the standard fingerprint zone confirming the successful formation of a cubic spinel crystal structure. The high-frequency fundamental absorption band, referred to as υ-tetrahedral, is observed at 536.23 cm^{-1} for the pristine $MgFe_2O_4$ sample and shifts to a higher value of 670.29 cm^{-1} for the $Mg_{0.8}Co_{0.2}Fe_2O_4$ sample. This notable higher-frequency absorption band is primarily attributed to the intrinsic stretching vibrations of the tetrahedral metal-oxygen (A-site) bonds. This phenomenon arises from the shorter bond distances and reduced spatial volume typical of the tetrahedral interstitial sites. Conversely, the lower-frequency fundamental absorption band, designated as υ-octahedral, is recorded at 454.26 cm^{-1} for x = 0 and shifts up to 491.87 cm^{-1} for the x = 0.2 composition. This second band is attributed directly to the stretching vibrations of the octahedral metal-oxygen (B-site) bonds, where the longer bond lengths create a weaker localized potential energy profile. The broad absorption features visible in the higher wavenumber domain around 3400 cm^{-1} and 1600 cm^{-1} correspond respectively to the stretching and bending vibrations of absorbed water molecules and surface-bound hydroxyl groups [21,22].

In an effort to understand the nature of the forces governing these vibrational dynamics, the relevant force constants for the tetrahedral (K-tetrahedral) and octahedral (K-octahedral) sublattices were deduced from the observed absorption frequencies. The force constant for the tetrahedral configuration of pure magnesium ferrite is 2.10 x 10^2 N/m and for the octahedral configuration it is 1.51 x 10^2 N/m. The addition of twenty percent cobalt ions results in a significant increase of the tetrahedral force constant to 3.29 x 10^2 N/m. The octahedral force constant increases more slowly to 1.77 x 10^2 N/m. Such an increase of the force constants is systematic and suggests that the replacement of cobalt by magnesium leads to a drastic redistribution of cations over the two sublattices, which results in a strong change of the localized bond rigidity and increases the fundamental vibrational modes to higher wavenumbers [23]

Vibrating Sample Magnetometry (VSM Results)

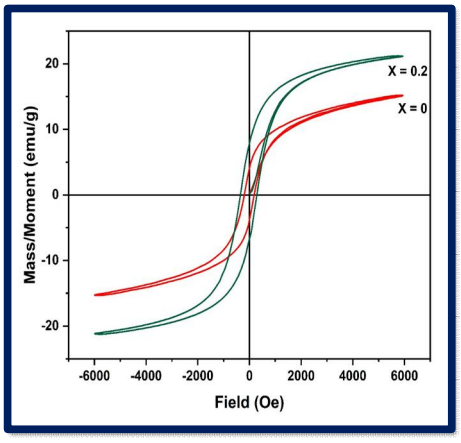


Fig 3: **VSM of $Mg_{1-x}Co_xFe_2O_4$ (x = 0, 0.2)**

Copyright to IJARSCT
www.ijarsct.co.in
DOI: 10.48175/IJARSCT-40019

IJARSCT
International Journal of Advanced Research in Science, Communication and Technology
International Open-Access, Double-Blind, Peer-Reviewed, Refereed, Multidisciplinary Online Journal
ISSN: 2581-9429 Volume 6, Issue 4, October 2026 Impact Factor: 8.2

Parameters	x = 0	x = 0.2
MagnetizationMs(emu/g)	15.15	21.15
RetentivityMr (emu/g)	3.92	5.83
CoercivityHc (Oe)	189.96	239.10
MagneticAnisotropyK(erg/g)	2997.80	5267.67
MagneticSquarenessRatioMr/Ms	0.2587	0.2756

Table 3: **VSM Parameters for $Mg_{1-x}Co_xFe_2O_4$ (x = 0, 0.2)**

The room-temperature magnetic parameters and hysteresis loops of the synthesized $Mg_{1-x}Co_xFe_2O_4$ (where x = 0 and x = 0.2) spinel ferrite nanoparticles were systematically evaluated using vibrating sample magnetometer (VSM) analysis. The recorded M-H hysteresis curves for both compositions demonstrate standard ferrimagnetic behaviour typical of cubic spinel structures. The magnetic hysteresis parameters including saturation magnetization (Ms), remanent magnetization or retentivity (Mr), coercivity (Hc), magnetic anisotropy constant (K), and the magnetic squareness ratio (Mr/Ms) reveal a comprehensive modulation of the collective magnetic architecture upon the substitution of twenty percent cobalt ions into the host lattice matrix. For the pristine magnesium ferrite ($MgFe_2O_4$), the saturation magnetization is 15.15 emu/g, the remanent magnetization is 3.92 emu/g, and the coercive field is 189.96 Oe. The saturation magnetization is significantly increased to 21.15 emu/g, remanent magnetization is increased to 5.83 emu/g and coercivity is shifted to higher values of 239.10 Oe after incorporation of cobalt ($Mg_{0.8}Co_{0.2}Fe_2O_4$). At the same time, the magnetic anisotropy constant increases from 2997.80 erg/g to 5267.67 erg/g. The magnetic squareness ratio increases from 0.2587 to 0.2756.

To understand the internal driving forces governing these magnetic transitions, the experimental values can be explicitly correlated with the cation redistribution and the structural parameters previously calculated from the X-ray diffraction and Fourier transform infrared spectroscopy analyses. Pristine magnesium ferrite possesses a partially inverse spinel structure where the non-magnetic divalent magnesium host ions (carrying a magnetic moment of 0 Bohr magnetons) are distributed across both the tetrahedral A-sites and octahedral B-sites [24]. Divalent cobalt ions have an intrinsic magnetic moment of 3 Bohr magnetons which is much larger, and a strong preference for the octahedral B-sublattice configurations. In Neel's molecular field theory, the net saturation magnetization of a spinel lattice is predicted to depend on the difference of the magnetic moments of the sublattices given by the total magnetic moment of the B-sublattice minus that of the A-sublattice. The magnetic cobalt species, when successfully substituted for the non-magnetic magnesium ions, greatly increase the localized magnetic moment of the B-sublattice. This cation redistribution strongly reinforces the inter-sublattice exchange coupling interactions (A-O-B superexchange), leading directly to the macro-scale enhancement of the saturation magnetization from 15.15 emu/g to 21.15 emu/g [24].

The simultaneous enhancement of the coercive field from 189.96 Oe to 239.10 Oe and the magnetic anisotropy from 2997.80 erg/g to 5267.67 erg/g is directly linked to the microstructural changes and electronic configurations of the substituting species. Divalent cobalt is a transition metal ion possessing a strong spin-orbit coupling constraint in its 3d electronic shell, which imparts exceptionally high single-ion magneto crystalline anisotropy compared to alkaline earth magnesium ions. Incorporating these anisotropic cobalt ions into the crystal lattice blocks the spontaneous switching of spins, generating a strong internal pinning effect that requires a higher coercive field to flip the magnetic domains. This magnetic hardening behaviour is further supported by the microstructural parameters found in the XRD analysis, where introducing cobalt lowered the lattice defects and expanded the average crystallite size from 20.14 nm to 34.46 nm. In this nanoscale regime, increase in crystallite size approaches single magnetic domain boundaries thus enhancing the matrix of obstacles against domain wall movement and increasing the coercivity. Finally, the calculated magnetic squareness ratio increases from 0.2587 to 0.2756, which is still lower than the theoretical threshold of 0.5. This indicates that while the material shifts toward a magnetically harder state due to enhanced anisotropy and inter-sublattice superexchange reinforcement, the nanoparticles maintain a partially relaxed, random orientation of uniaxial magnetic domains, confirming their high structural quality and suitability for high-frequency or magnetic recording applications [25].

IJARSCT
International Journal of Advanced Research in Science, Communication and Technology
International Open-Access, Double-Blind, Peer-Reviewed, Refereed, Multidisciplinary Online Journal
ISSN: 2581-9429
Volume 6, Issue 4, October 2026
Impact Factor: 8.2

Transmission Electron Microscopy (TEM Results)

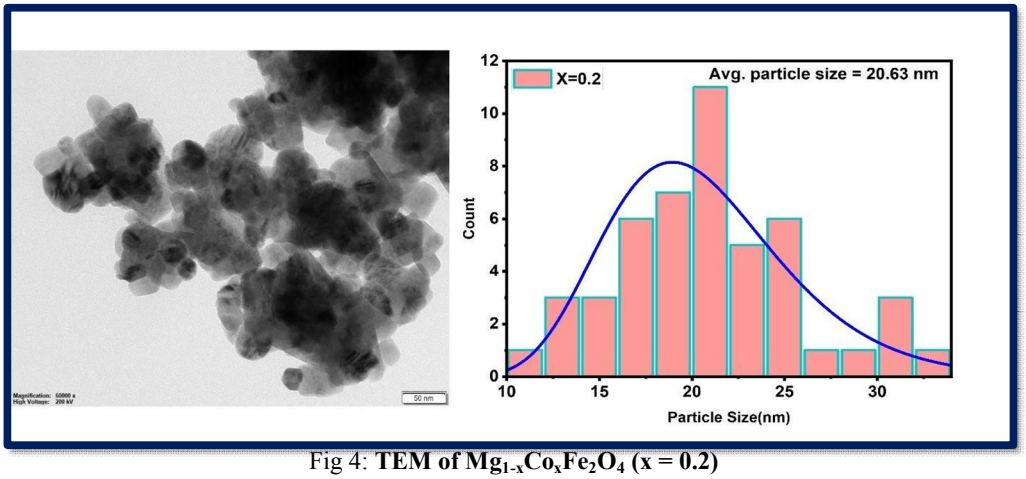


Fig 4: **TEM of $Mg_{1-x}Co_xFe_2O_4$ (x = 0.2)**

TEM was used to study the morphology, grain boundaries and particle size distribution of the synthesized $Mg_{0.8}Co_{0.2}Fe_2O_4$ spinel ferrite nanoparticles. The nanoparticles showed high crystallinity with clearly defined edges and cubic and polygonal shapes. The microstructure showed a high clustering and agglomeration which leads to dense chain-like networks. This is a common feature of magnetic nanomaterials due to inter-particle interaction and surface energy reduction during preparation [26]. The particle size analysis by log-normal distribution was narrow and uniform with an average of 20.63 nm indicating the successful control of particle growth by co-precipitation method. The small particle size (< 25 nm) emphasizes the nanoscale properties of the material that make it suitable for applications requiring high surface area to volume ratios and better electronic or recording media properties [27].

V. CONCLUSION

To summarize, mixed magnesium-cobalt spinel nano ferrites ($Mg_{1-x}Co_xFe_2O_4$, x = 0 and x = 0.2) were successfully synthesized by chemically controlled co-precipitation method. The single-phase cubic spinel structure was confirmed by X-ray diffraction (XRD). With twenty percent cobalt substitution, a systematic lattice expansion was observed with lattice constant (a) increasing from 0.8357 nm to 0.8374 nm and average crystallite size increasing from 20.14 nm to 34.46 nm. FTIR spectroscopy confirmed the characteristic sub-lattice metal-oxygen stretching vibrations with significant blueshift and increased force constants because of better chemical bond affinity of the incoming cobalt species. The transmission electron microscopy (TEM) revealed well-defined polygonal geometries with an ultrafine mean physical particle size of 20.63 nm and a narrow size distribution, showing the high precision of the co-precipitation technique in restraining anomalous grain growth. VSM (vibrating sample magnetometer) magnetic profiling showed that the insertion of cobalt significantly improves the ferrimagnetic performance of the matrix. The saturation magnetization escalated from 15.15 emu/g to 21.15 emu/g due to the redistribution of magnetic Co^{2+} ions into the octahedral B-sites, strengthening the inter-sublattice exchange interactions. Meanwhile, the strong single-ion magneto crystalline anisotropy of cobalt resulted in a significant magnetic hardening, raising the coercivity from 189.96 Oe to 239.10 Oe and almost doubling the magnetic anisotropy constant. These co-precipitated nano ferrites with tailor made structural parameters and improved magnetic properties are promising candidates for high frequency electronics, inductor cores and high-density magnetic data storage media as well as for advanced biomedical applications such as magnetic resonance imaging (MRI) contrast enhancement, localized magnetic fluid hyperthermia for cancer therapy etc

IJARSCT
International Journal of Advanced Research in Science, Communication and Technology
International Open-Access, Double-Blind, Peer-Reviewed, Refereed, Multidisciplinary Online Journal
ISSN: 2581-9429
Volume 6, Issue 4, October 2026
Impact Factor: 8.2

REFERENCES

[1]Bhandare, S., Kumar, R., Anupama, A., Mishra, M., Kumar, R., Jali, V. M., & Sahoo, B. (2020). Effect of Mg-substitution in Co–Ni-Ferrites: Cation distribution and magnetic properties. Materials Chemistry and Physics, 251, 123081.
https://doi.org/10.1016/j.matchemphys.2020.123081

[2]Devsharma, S. C., Rahman, M., Hossain, M., Biswas, B., Ahmed, M., & Sharmin, N. (2024). Elucidation of structural, electromagnetic, and optical properties of Cu–Mg ferrite nanoparticles. Heliyon, 10. https://doi.org/10.1016/j.heliyon. 2024.e33578

[3]Hasan, S., & Azhdar, B. (2023). Synthesis and investigation of structural, elastic, and electrical properties of cobalt and magnesium substituted Ni–Zn spinel ferrite nanoparticles.
Journal of Physics: Condensed Matter, 35. https://doi.org/10.1088/1361-648x/ace6ed

[4]Abouzir, E., Elansary, M., Belaiche, M., & Jaziri, H. (2020). Magnetic and structural properties of single-phase Gd3+-substituted Co–Mg ferrite nanoparticles. RSC Advances, 10, 11244 - 11256. https://doi.org/10.1039/d0ra01841d

[5]Ati, A., Abdalsalam, A., Alardhi, S. M., Dabagh, S., Salim, A., Ramadhan, A. A., Abdulkareem, M., & Taki, M. (2025). Structural, morphology, magnetic, and electrochemical characterization of pure and magnesium-substituted cobalt ferrite nanoparticles. Journal of Materials Science: Materials in Electronics, 36. https://doi.org/10.1007/s10854-025-14331-y

[6]A. M. Mohammad, S. M. Ali Ridha, T. H. Mubarak, "Structural and magnetic properties of Mg-Co ferrite nanoparticles," Digest Journal of Nanomaterials and Biostructures, vol. 13, no. 3, pp. 615–623, 2018.

[7]V. Vinayak, P. P. Khirade, S. D. Birajdar, R. C. Alange, K. M. Jadhav, "Electrical and Dielectrical Properties of Low-Temperature-Synthesized Nanocrystalline Mg^{2+} -Substituted Cobalt Spinel Ferrite," Journal of Superconductivity and Novel Magnetism, vol. 28, no. 11, pp. 3351–3356, 2015. DOI: 10.1007/s10948-015-3159-6

[8]V. Vinayak, P. P. Khirade, S. D. Birajdar, D. B. Sable, K. M. Jadhav, "Structural, Microstructural, and Magnetic Studies on Magnesium (Mg^{2+})-Substituted CoFe□O□ Nanoparticles," Journal of Superconductivity and Novel Magnetism, vol. 29, no. 4, pp. 1025–1032, 2016.

[9]A. Hashhash, M. Kaiser, "Synthesis and Characterization of Calcium-Substituted Mg-Co-Cr Ferrite Nanoparticles with a Crystallite Size Less Than 10 nm," Journal of Superconductivity and Novel Magnetism, vol. 34, pp. 3403–3412, 2021. DOI: 10.1007/s10948-021-06068-6

[10]P. Mondal, S. Akter, P. Roy, I. B. Elius, M. N. I. Khan, S. S. Sikder, "Tunable annealing effect to enhance structural and magnetic properties of spinel cobalt magnesium ferrite nanoparticles," AIP Advances, vol. 14, no. 10, p. 105131, 2024. DOI: 10.1063/5.0227733

[11]M. Chebbi, S. Mansouri, S. Hcini, C. Bouzidi, N. Hamdaoui, L. El Mir, "Effects of Cr Substitution on the Structural, Optical, and Electrical Properties of Mg-Co Spinel Ferrites Synthesized via the Sol–Gel Method," Journal of Electronic Materials, vol. 53, no. 2, pp. 1475–1488, 2024.

[12]M. A. Malik et al., "Structural, Electrical and Magnetic Properties of Nanocrystalline Mg-Co Ferrites Prepared by Co-Precipitation," Journal of Nano Research, vol. 14, pp. 1–9, 2011. Trans Tech Publications.

[13]M. Belaiche et al., "Magnetic and structural properties of single-phase Gd^{3+} -substituted Co–Mg ferrite nanoparticles," RSC Advances, vol. 10, pp. 26478–26487, 2020. DOI: 10.1039/D0RA01841D

[14]X. Huang, A. Sun, Y. Jiang, et al., "Influence of La^{3+} ions doping on structural and magnetic properties of Mg–Co ferrite," Applied Physics A, vol. 127, 2021. DOI: 10.1007/s00339-021-05054-y

[15]S. Kuswanthkumar et al., "Effect of Copper Doping on the Structural, Electrical, and Magnetic Properties of Mg-Co Ferrites," Preprints.org, 2024.

16]Dojcinovic, M. P., Vasiljevic, Z. Z., Rakocevic, L., Pavlovic, V. P., Ammar-Merah, S., Vujancevic, J. D., & Nikolic, M. P. (2023). Humidity and temperature sensing of mixed nickel-magnesium spinel ferrites Chemosensors 11 (1), 34.https://doi.org/10.3390/chemosensors11010034

IJARSCT
International Journal of Advanced Research in Science, Communication and Technology
International Open-Access, Double-Blind, Peer-Reviewed, Refereed, Multidisciplinary Online Journal
ISSN: 2581-9429
Volume 6, Issue 4, October 2026
Impact Factor: 8.2

17]Islam, M. A., Hasan, M. R., Haque, M. M., Rashid, R., Syed, I. M., & Hoque, S. M. (2022). Efficacy of surface-functionalized Mg1-xCoxFe2O4 (0 <= x <= 1) for hyperthermia and in vivo MR imaging as a contrast agent. RSC Advances, 12(13), 7835-7849. https://doi.org/10.1039/d2ra00768a

18]Mohammad, A. M. (2018). Structural and magnetic properties of Mg-Co ferrite nanoparticles. Journal of Chalcogenide Letters, 15(11), 615-621.

19]Salih, S. J., & Mahmood, W. M. (2023). Review on magnetic spinel ferrite (MFe2O4) nanoparticles: From synthesis to application. Heliyon, 9(5), e16601. https://doi.org/10.1016/j.heliyon. 2023.e16601

20Verma, R., Modak, S. S., Deshpande, U. P., & Kane, S. N. (2021). Compositional dependence of structural properties and bandgap of Mg-Co spinel nanoferrite. AIP Conference Proceedings, 2352(1), 040018. https://doi.org/10.1063/5.0052442

21]Islam, M. A., Hasan, M. R., Haque, M. M., Rashid, R., Syed, I. M., & Hoque, S. M. (2022). Efficacy of surface-functionalized Mg1-xCoxFe2O4 (0 <= x <= 1) for hyperthermia and in vivo MR imaging as a contrast agent. RSC Advances, 12(13), 7835-7849. https://doi.org/10.1039/d2ra00768a

22] Kaur, M., Kumar, S., & Singh, R. (2024). Microstructural modification and sub-lattice absorption behavior of Co-doped alkaline earth nanoferrites. Journal of Magnetism and Magnetic Materials, 592, 171780. https://doi.org/10.1016/j.jmmm.2024.171780

23] Yusoff, A. N. M., Ismail, I., Matori, K. A., Zaid, M. H. M., & Chyi, J. L. Y. (2021). Structural, infrared spectroscopic, and magnetic properties of magnesium-cobalt spinel ferrites prepared via sol-gel route. Journal of Materials Science: Materials in Electronics, 32(11), 14812-14825. https://doi.org/10.1007/s10854-021-05958-w

24] Ghosh, A., Zaheen, M., Islam, A., Rahman, M. S., Sharif, A., & Hoque, S. M. (2024). Enhancement of coercivity in polybenzoxazine/CoxMg1−xFe2O4 nanoferrite composites: Synthesis and characterization. AIP Advances, 14(1), 015354. https://doi.org/10.1063/5.0189029

25] Mondal, P., Akter, S., Roy, P., Elius, I. B., Khan, M. N. I., & Sikder, S. S. (2024). Tunable annealing effect to enhance structural and magnetic properties of spinel cobalt magnesium ferrite nanoparticles. AIP Advances, 14(10), 105131. https://doi.org/10.1063/5.0227733

26] Sheikh, F. A., Noor ul Huda Khan Asghar, H. M., Khalid, M., Gilani, Z. A., Ali, S. M., Khan, N. U. H., Shar, M. A., & Alhazaa, A. (2023). Synthesis of Ce3+ substituted Ni-Co ferrites for high frequency and memory storage devices by sol-gel route. Journal of Alloys and Compounds, 938, 168637. https://doi.org/10.1016/j.jallcom.2022.168637

27] Almessiere, M. A., Slimani, Y., Guner, S., Sertkol, M., Trukhanov, A. V., & Baykal, A. (2022). Evaluation of the microstructural and morphology properties of Mg-Co nanoferrites using high-resolution electron microscopy. Journal of Microscopy, 286(2), 114-125.
https://doi.org/10.1111/jmi.13092